Cyclization Increases the Antimicrobial Activity and Selectivity of Arginine- and Tryptophan-Containing Hexapeptides†

Margitta Dathe,* Heike Nikolenko, Jana Klose, and Michael Bienert

Institute of Molecular Pharmacology, Robert-Roessle-Strasse 10, D-13125 Berlin, Germany

Received October 31, 2003; Revised Manuscript Received May 12, 2004

ABSTRACT: Arginine- and tryptophan-rich motifs have been identified in antimicrobial peptides with various secondary structures. We synthesized a set of linear hexapeptides derived from the sequence AcRRWWRF-NH_2 by substitution of tryptophan (W) by tyrosine (Y) or naphthylalanine (Nal) and by replacement of arginine (R) by lysine (K) to investigate the role of cationic charge and aromatic residues in membrane activity and selectivity. A second set of corresponding head-to-tail cyclic analogues was prepared to analyze the role of conformational constraints. The biological activity of the linear peptides followed the order Nal- ≫ W- > Y-containing compounds and slightly decreased upon R−K substitution. A pronounced activity-improving and bacterial selectivity-enhancing effect was found upon cyclization of the R- and W-bearing parent peptide, whereas the activity-modifying effect of cyclization of Y- and Nal-containing peptides was low. The analysis of the driving forces of peptide interaction with model membranes showed that the activities correlated with the partition coefficients and the depths of peptide insertion into neutral and negatively charged lipid bilayers. Spectroscopic studies, RP-HPLC, and titration calorimetry implied that the combination of cationic and aromatic amino acid composition and conformational rigidity afforded a membrane-active, amphipathic structure with a highly charged face opposed by a cluster of aromatic side chains. However, threshold values of low and high hydrophobicity seemed to exist beyond which the activity-enhancing effect of cyclization was negligible. The results suggest that cyclization of small peptides of an appropriate amino acid composition may serve as a promising strategy in the design of antimicrobial peptides.

Antimicrobial peptides are important components of the animal defense against microbial infections (*1*). Many peptides possess a broad spectrum of activity against microorganisms by interacting with the bacterial envelope and altering the permeability of the target membrane (*2*). The peptide structure accounts for this mode of action. Most peptides bear cationic charges which initiate accumulation preferentially at the negatively charged bacterial surface. Additionally, they display or may form domains of hydrophobic residues which permit insertion into the nonpolar interior of the lipid matrix of cell membranes. Subsequent formation of pores or global disturbance of the lipid arrangement have been suggested to lead finally to cell death (*3*).

The interest in antimicrobial peptides is stimulated by the possibility to use them as substitutes for conventional antibiotics against which many bacteria have developed resistance. Besides unresolved problems of toxicity against eukaryotic cells and limited stability, high production costs render large peptides not very promising as drug leads. Thus, it is important to develop smaller antimicrobial peptides with improved stability. However, unlike many amphipathic helical peptides and β-sheet structures, only a few small microbicidal peptides have been described. Substantial antimicrobial activity was found for a lactoferricin-derived hexapeptide (*4*), truncated analogues of indolicidin (*5*), or hexapeptides derived from tritrypticin (*6*). All these peptides are rich in tryptophan (W) and arginine (R). Using synthetic combinatorial libraries, AcRRWWRF-NH_2 has been identified as a sequence active against different bacterial strains and yeast cells (*7*). Recently, R- and W-containing antimicrobial pentapeptides (*8*) and even dipeptides have been described (*9*). R- and W-rich motifs similar to the six-residue antibiotic core peptide of bovine lactoferricin have also been found in conformationally constrained antimicrobial peptides such as polyphymesin I (*10*) and tachyplesin I (*11*).

How short peptides can exert potent antimicrobial activity and which role R- and W-rich sequence motifs and their conformation play in large peptides have been investigated very little (*12*). Aromatic residues modulate the biological activity of several hemolytic and antimicrobial peptides. Thus, substitution of the two W residues by phenylalanine (F) in a lactoferricin peptide resulted in the loss of activity, whereas introduction of more hydrophobic residues improved the antimicrobial effect (*13*). More potent analogues were generated by introduction of W into cyclic bactenicin (*14*), whereas W exchange by Y in indolicidin reduced both the antimicrobial and hemolytic effects (*5*). Arginine residues have been found to be the sole or main cationic residues in several antimicrobial peptides such as protegrins (*15*), bactenecin (*16*), or PR-39 (*17*). The relevance of R for the activity of small peptides was demonstrated by less potent K-containing analogues of an 11-residue lactoferricin seg-

† This study was supported by Grant DA 324/4-1 of the Deutsche Forschungsgemeinschaft.

* To whom correspondence should be addressed. Phone: 030 94 793 274. Fax: 030 94 793 159. E-mail: dathe@fmp-berlin.de.

10.1021/bi035948v CCC: $27.50
Published on Web 06/25/2004

ment (*18*). In contrast, the arginine side chain played a minor role in indolicidin activity as replacement of R by lysine or ornithine had negligible effects (*5*). Van't Hof analyzed the relationship between the secondary structure and the activity of lactoferrin and truncated analogues bearing the sequence RRWQWR (*19*). This motif, in which the putative antimicrobial activity is located, exists in lactoferrin as an α-helix. In lactoferricin B, the sequence is present in a β-structure (*20*), and the very active synthetic hexapeptide adopts an unconventional structure (*21*). The chemical homology and structural variability of the RW-rich motif raised the question of whether the specific amino acid residues were responsible for the effect independent of the secondary structure, or whether the small sequences fulfilled the organizational principles of amphipathicity and membrane activity.

Our studies on helical amphipathic peptides have shown that peptide activity and selectivity toward cell membranes and lipid bilayers are less dependent on the amino acid composition but determined by global structural parameters of the peptides and by the properties of the target membrane (*22*, *23*). In this paper we present a study of short peptides based on the linear sequence AcRRWWRF-NH_2. Which role do tryptophan and arginine play in membrane activity and selectivity, and how do conformational constraints influence the biological effects? To answer these questions, we synthesized linear and head-to-tail cyclic analogues with arginine (R) replaced by lysine (K) and with tyrosine (Y) or naphthylalanine (Nal) introduced for tryptophan (W). We determined antimicrobial and hemolytic activities and analyzed the peptide effect on negatively charged and neutral lipid bilayers to see which role interactions with the lipid matix of the target membranes play in the biological effects. The studies showed that conformational rigidity of the R- and W-bearing peptides induced by cyclization was a suitable method for inducing pronounced antimicrobial activity and selectivity. We propose that clustering of the aromatic residues and increasing the cationic charge density by cyclization enhanced amphipathicity and provided the basis for high membrane activity. Threshold values of low and high global hydrophobicity seemed to exist below and above which the activity-enhancing effect of cyclization was eliminated. A preliminary account of this work has been presented (*24*).

MATERIALS AND METHODS

Materials. The lipids 1-palmitoyl-2-oleoylphosphatidylcholine (POPC),[1] 1-palmitoyl-2-oleoylphosphatidyl-*sn*-glycerol (POPG), 1-palmitoyl-2-stearyl(5-doxyl)-*sn*-glycero-3-phosphatidylcholine (5-DOX), 1-palmitoyl-2-stearyl(12-doxyl)-*sn*-glycero-3-phosphatidylcholine (12-DOX), and 1,2-dioleoyl-*sn*-glycero-3-phosphotempocholine (TEMPO) were purchased from Avanti Polar Lipids, Inc., Alabaster, AL. Acryalmide was from SERVA, Germany. Calcein was obtained from Fluka Chemie, Germany, and tris(hydroxymethyl)aminomethane (Tris) and other chemicals used in biophysical experiments were from Merck, Germany. Luria broth (LB) was obtained from Gibco BRL, Scotland.

Peptide Synthesis and Characterization. The linear peptides were synthesized automatically by the solid-phase method using standard Fmoc chemistry in the continuous-flow mode on a MilliGen 9050 peptide synthesizer (Millipore) (*25*). Cyclization of linear sequences was done manually by applying HAPyU chemistry (*26*). The peptides were purified by preparative reversed-phase high-performance liquid chromatography (RP-HPLC) using a Shimadzu LC-10AD system operating at 220 nm to give final products more than 95% pure by HPLC analysis. The compounds were further characterized by matrix-assisted laser desorption mass spectrometry (MADLI II, Kratos, U.K.). Chromatographic characterization was performed on a Jasco HPLC system (Japan) with a diode array detector operating at 220 nm. Runs were carried out on a PolyEncap A 300 (250 × 4.0 mm) column (Bischoff Analysentechnik, Germany). The sample concentration was 1 mg/mL peptide in eluent A. Mobile phase A was 0.1% trifuoroacetic acid in water, and B was 0.1% trifuoroacetic acid in 80% acetonitrile/20% water (v/v). The retention times (t_R) of the peptides were determined using a linear gradient of 5−95% B over 40 min at 22 °C.

Preparation of Small and Large Unilamellar Vesicles. Vesicles for spectroscopic and titration calorimetric measurements were prepared and characterized as described elsewhere (*22*). SUVs were made by vortex mixing of dried lipid in buffer (10 mM Tris, 154 mM NaCl or NaF for spectroscopic measurements, 0.1 mM EDTA, pH 7.4) and sonicating. Dynamic light scattering measurements (N4 Plus, Coulter Corp.) confirmed the existence of a main population of vesicles (more than 95% mass content) with a mean diameter of 45 ± 2 nm (polydispersity index 0.3). Calcein-containing LUVs were prepared by vortexing the dried lipid in dye buffer solution (70 mM calcein, 10 mM Tris, 0.1 mM EDTA, pH 7.4). The suspension was frozen−thawed in liquid nitrogen for eight cycles and extruded **(**Lipex Biomembranes Inc., Canada) through polycarbonate filters (six times through two stacked 0.4 μm pore size filters followed by eight times through two stacked 0.1 μm pore size filters). Untrapped calcein was removed using a minicolumn centrifugation method (*27*). The lipid concentration was determined by phosphorus analysis (*28*).

Quenching Studies. POPC and mixed POPC/POPG (3/1 mol/mol) vesicles with different amounts of nitroxide spin-labeled lipids were prepared by mixing appropriate volumes of POPC, POPG, and labeled lipid dissolved in chloroform and subsequent drying under nitrogen. The peptides were dissolved in ethanol to give a final concentration of 200 μM. A 20 μL sample of the peptide solution was added to the lipid-containing tube to dissolve the lipid film followed by vortex mixing with 1980 μL of buffer (10 mM Tris, 154 mM NaCl, 0.1 mM EDTA, pH 7.4). The final concentrations were 200 μM lipid and 2 μM peptide, and the content of labeled lipid ranged from 0 to 40 mol %. Solutions for baseline samples lacked peptide. The tryptophan fluorescence excited at 285 nm was measured with an LS 50B

[1] Abbreviations: cfu, colony-forming unit; DMSO, dimethyl sulfoxide; 5-DOX, 1-palmitoyl-2-stearyl(5-doxyl)-*sn*-glycero-3-phosphatidylcholine; 12-DOX, 1-palmitoyl-2-stearyl(12-doxyl)-*sn*-glycero-3-phosphatidylcholine; TEMPO, 1,2-dioleoyl-*sn*-glycero-3-phosphotempocholine; CD, circular dichroism; EDTA, ethylenediaminetetraacetic acid; HAPyU, *O*-7-(azobenzotriazol-1-yl)-1,1,3,3-(bis(tetramethylene)-uronium) hexafluorophosphate; LB, Luria broth; LPS, lipopolysaccharide; LUVs, large unilamellar vesicles; MIC, minimum inhibitory concentration; POPC, 1-palmitoyl-2-oleoyl-*sn*-glycero-3-phosphatidylcholine; POPG, 1-palmitoyl-2-oleoyl-*sn*-glycero-3-(phospho-*rac*-(glycerol)); RP-HPLC, reversed-phase high-performance liquid chromatography; SUVs, small unilamellar vesicles; SDS, sodium dodecyl sulfate; Tris, tris(hydroxymethyl)aminomethane.

spectrofluorimeter (Perkin-Elmer Corp., Germany) at the emission maximum of 344 nm. Quenching is given by $F/F_o = \exp(-\Pi(c/70)(R_o^2 - X^2 - z^2))$, where F_o and F are the fluorescence intensities in the absence and presence of the quencher, respectively, R_o is the critical quenching distance of the W−doxyl pair (12 Å) (*29*), X is the minimum allowed lateral distance between the fluorophore and quencher, z is the difference in depth between the quencher and fluorophore, c is the mole fraction of the quencher molecule, and $c/70$ gives the number of quencher molecules per square angstrom assuming that the cross-sectional area of a lipid is 70 Å^2. The distance of tryptophan from the bilayer center, z_{cf}, was calculated using the parallax equation $z_{cf} = L_{c1} + (-70/\Pi c(\ln(F_1/F_2) - L_{21}^2))/2L_{21})$, with L_{c1} being the distance of the shallow quencher from the bilayer center, F_1 and F_2 the fluorescence intensities in the presence of the shallow and deeper quenchers, respectively, and L_{21} the difference in depth between the shallow and deeper quenchers (*30*). The distances of the applied quenching groups from the bilayer center have been reported to be 19.5 Å for TEMPO (*31*) and 12.2 and 5.85 Å for 5-DOX and 12-DOX, respectively (*30*).

The ability of acrylamide to quench the tryptophan fluorescence of peptides in buffer (10 mM Tris, 154 mM NaCl, 0.1 mM EDTA, pH 7.4) and in the presence of SUV suspensions was studied by addition of increasing amounts of the quencher (4 M in buffer). The final peptide concentration was 5 μM, and the lipid concentration reached 2.5 mM. The emission spectra (excitation at 280 nm) were corrected for dilution as well as the inner-filter effect and light scattering according to the relation $F_{corr} = F \times 10^{(A_{\lambda ex} + A_{\lambda em}) \times 0.5}$, with $A_{\lambda_{ex}}$ and $A_{\lambda_{em}}$ being the absorbances at the wavelengths of excitation and the emission maximum. Assuming that a fraction of lipid-bound peptides is inaccessible to the quencher, the Stern−Volmer quenching constants (K_{SV}) and the fraction of peptide (f) accessible to acrylamide were evaluated by curve fitting using the equation $F/F_o - 1 = (K_{SV}c_q f)/(1 + K_{SV}c_q(1 - f))$ (*32*), where c_q is the quencher concentration.

Circular Dichroism Measurements. CD measurements of 100 μM buffered peptide solutions (10 mM Tris, 154 mM NaF, pH 7.4) in 25 mM SDS solution and in 10 mM POPG SUV suspensions were carried out on a J 720 spectrometer (Jasco, Japan) at room temperature. Circular dichroism and differential scattering of the SUVs were eliminated by subtracting the spectra of the corresponding peptide-free lipid suspensions. The spectra presented give the mean residue ellipticity [Θ] of one out of two independent experiments.

Peptide-Induced Dye Release from Liposomes. Peptide-induced calcein release from vesicles was monitored fluorimetrically by measuring the decrease in self-quenching as a function of time after adding an aliquot of an LUV suspension to the peptide solution as described (*22*). The peptide concentration ranged between 1 and 100 μM, and the lipid concentration was 25 μM. The fluorescence was excited at 490 nm and registered at 520 nm on an LS 50B spectrofluorimeter (Perkin-Elmer Corp., Germany). The fluorescence intensity corresponding to 100% dye release was determined by addition of Triton X-100 (10% v/v in water).

Peptide Binding. Isothermal titration calorimetry was performed using a VP isothermal titration calorimeter (MicroCal Inc., Norhampton, MA). Experiments were made with SUVs at $T = 25$ °C. Into the peptide solution (concentration $c_p = 40$ or 80 μM) in the calorimeter cell were injected aliquots of an SUV suspension (20 μL; lipid concentration $c_l = 44$ mM). The measured heat of peptide binding decreased with consecutive lipid injections because of the gradual reduction in free peptide. As a control, the phospholipid suspension was injected into buffer. A heat of dilution of about −11 μcal was determined. From the sum of the heat of injections, the reaction enthalpy, $\Delta H°$, was calculated. The cumulative heat of reaction as a function of the number of injections was used to calculate binding isotherms. The evaluation of such data sets has been explained elsewhere (*33*). Binding of the cationic peptides to SUVs can be described by a surface partition equilibrium with the condition that the extent of peptide adsorption is linearly related to the peptide concentration at the vesicle surface, c_M: $R = Kc_M$. R is the molar amount of peptide bound per mole of lipid, and K is the partition coefficient. c_M is dependent on the free peptide concentration in the bulk solution, on the peptide charge, and on the membrane surface potential, which can be calculated with the aid of the Gouy−Chapman theory (for a review see ref *34*). Combining the binding model, Boltzmann relation, and Gouy−Chapman theory, it is possible to calculate c_M from the experimental binding data and to determine K. A detailed description of the binding model can be found elsewhere (*35*, *36*).

Hemolytic Assay. The hemolytic activity of the peptides was determined using human red blood cells (Blutspendedienst Deutsches Rotes Kreuz) as described previously (*22*). Suspensions containing the peptide at a concentration of 100 μM and 1.8×10^8 cells/mL were incubated for 30 min at 37 °C. After centrifugation an aliquot of the supernatant was dissolved in 0.5% NH_4OH, and the optical density (OD) was measured at 540 nm (Lambda 9 spectrophotometer, Perkin-Elmer Corp., Germany). Zero hemolysis (OD_0) and 100% hemolysis (OD_{100}) were determined using the supernatants of cell suspensions incubated in buffer and 0.5% NH_4OH, respectively. Values determined in repeated experiments differed by less than 5%.

Antibacterial Studies. Gram-negative *Escherichia coli* (DH 5α strain) and Gram-positive *Bacillus subtilis* (PY 22 strain) were used to test the antibacterial activity of the peptides (*23*). Bacteria were cultivated in LB at 37 °C with shaking at 180 rpm. The inoculum was prepared from mid-logarithmic-phase cultures ($OD_{600} = 0.5$). Aliquots of the cell suspensions were added to the wells of a microtiter plate containing peptide at different concentrations. The final concentration of bacteria was 10^5 cfu's/mL. The final concentrations of peptide ranged from 0.05 to 100 μM in 2-fold dilutions. Peptides were tested in duplicate. The microtiter plates were incubated overnight at 37 °C, and the absorbance was read at 600 nm (Autoreader EL 311, Bio-Tek Instruments Inc.). The minimum inhibitory concentration (MIC) is defined as the lowest concentration of peptide at which there was no change in optical density.

RESULTS

Biological Activity. Figure 1 illustrates the growth-inhibiting activity of linear and cyclic peptides (Table 1) toward Gram-negative *E. coli* and Gram-positive *B. subtilis*. Whereas

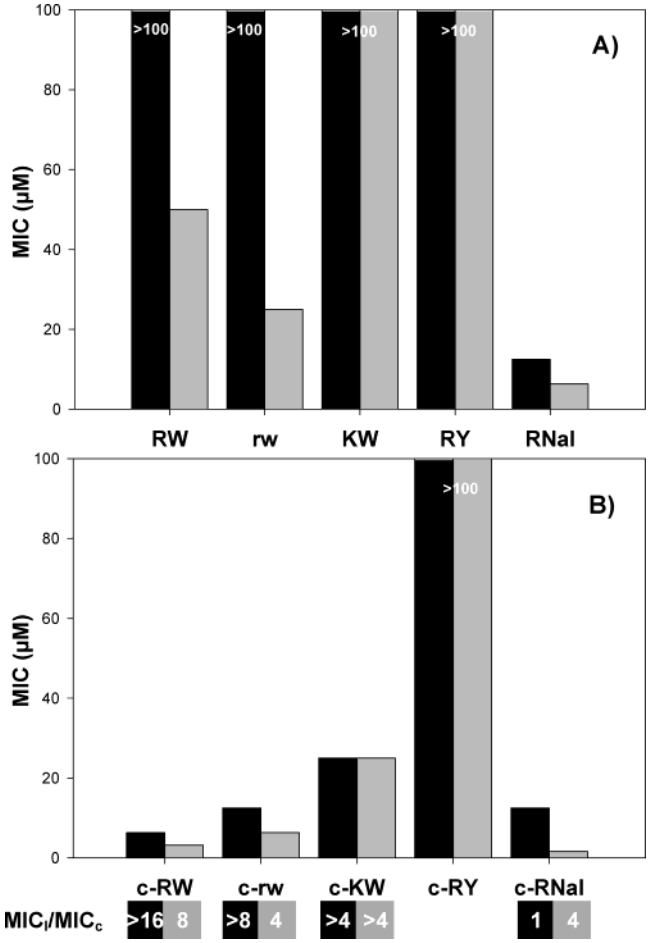

FIGURE 1: Antimicrobial activity of linear (A) and cyclic (B) hexapeptides. Shown is the MIC of the growth of *E. coli* (black bars) and *B. subtilis* (gray bars) (10^5 cfu's/mL). Triplicate values of two different experiments differed at most in one dilution step. MIC$_l$/MIC$_c$ gives the ratio of the MIC of the linear and corresponding cyclic peptide and is a measure for cyclization-induced improvement of the activity toward *E. coli* (black) and *B. subtilis* (gray).

Table 1: Amino Acid Sequences of Peptides, Abbreviations, and RP-HPLC Retention Times[a]

	linear[b]		cyclic	
peptide	name	t_R (min)	name	t_R (min)
RRWWRF	RW	17.7	c-RW	18.4
rrwwrf	rw	17.8	c-rw	18.4
KKWWKF	KW	16.3	c-KW	17.1
RRYYRF	RY	12.6	c-RY	12.4
RRNalNalRF	RNal	20.8	c-RNal	21.0

[a] t_R = RP-HPLC retention time. Small letters stand for D-amino acid residues. Nal = β-(naphth-1-yl)alanine. [b] N-terminally acetylated and C-terminally amidated.

the bacteria were not or only slightly susceptible to the linear sequences (Figure 1A) (except the Nal-bearing analogue) up to concentrations of 100 μM, cyclization of the W-containing peptides was connected to a substantial increase in the activity (Figure 1B). As shown by the quotient MIC$_l$/MIC$_c$ > 16, the activity-enhancing effect of cyclization was most pronounced for *E. coli*. The cyclic c-RY was as inactive as RY, and the antimicrobial effect of c-RNal was only slightly improved compared to that of the highly active linear analogue. All linear sequences showed low hemolytic activity at 100 μM concentration. Peptide-induced lysis of red blood

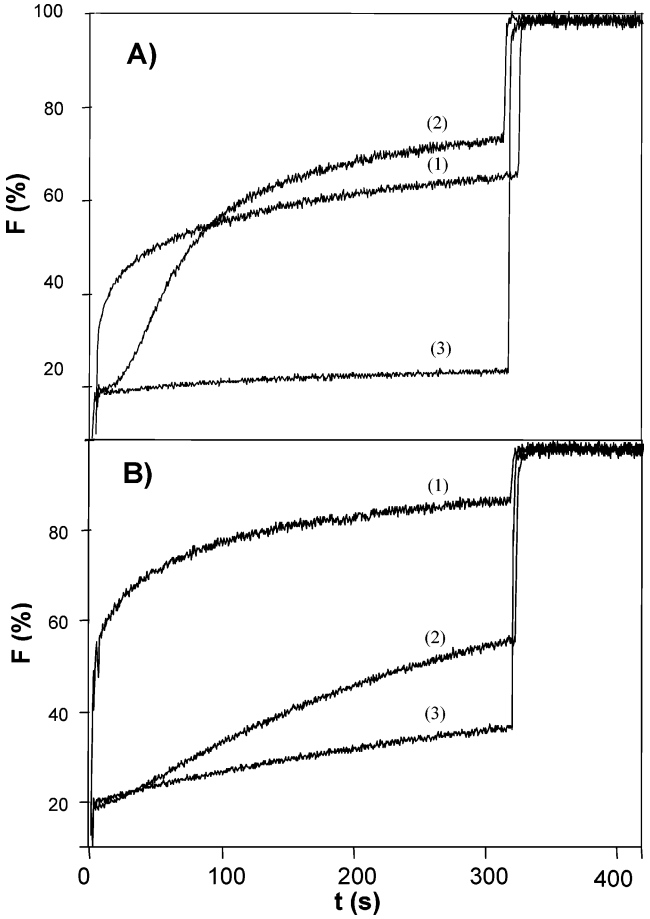

FIGURE 2: Kinetics of vesicle permeabilization. Dequenching of the calcein fluorescence (F) induced by RW (A) and c-RW (B) from POPC (1), POPG (2), and mixed POPC/POPG (3/1 mol/mol) LUVs as a function of time t. The lipid concentration, c_l, was 25 μM, and the peptide concentration, c_p, was 10 μM in buffer (10 mM Tris, 154 mM NaCl, 0.1 mM EDTA, pH 7.4). Total dequenching was induced after 5 min by addition of Triton X-100.

cells followed the order RNal (24%) > RW (7%) = rw (7%) > KW (4%) > RY (1%), and was enhanced by a factor of up to 3 upon cyclization. The activity patterns against bacteria and erythrocytes revealed that the cyclic W- and R-containing peptides were potent and selective antimicrobial compounds.

Peptide-Induced Dye Release from Liposomes. Although there existed differences in the permeabilization kinetics of the lipid bilayers as shown for RW (Figure 2A), the dye-releasing activities of linear peptides with highly negatively charged POPG and neutral POPC bilayers were comparable (Figure 3A, Table 2). The activity followed the order RNal > RW = rw > KW > RY. Cyclization enhanced the effect on POPC but reduced the effect on highly negatively charged model membranes (Figures 2B and 3B). Peptide activity toward mixed bilayers was low, with POPC/POPG (1/1 mol/mol) being most resistant (Table 2). The EC_{25} values of RW and c-RW show that the activity-enhancing effect of cyclization was pronounced on neutral and slightly negatively charged lipid layers but disappeared on POPG membranes.

Hydrophobicity and Amphipathicity As Determined by HPLC. Peptide hydrophobicity was characterized by retention times t_R in RP-HPLC (Table 1). The method monitors the affinity of compounds to the hydrophobic surface of the HPLC solid phase and has been successfully applied to characterize amphipathic helices (*37*) and β-structured pep-

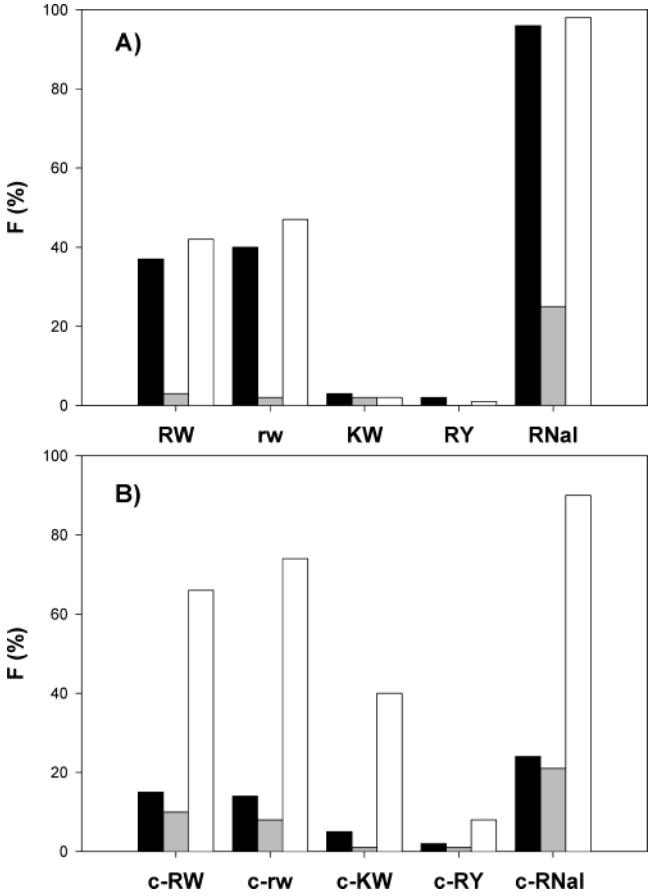

FIGURE 3: Bilayer-permeabilizing activity of linear (A) and cyclic (B) hexapeptides. Presented is the percentage of dequenching of the fluorescence (*F*) of calcein entrapped in LUVs composed of POPG (black bars), mixed POPC/POPG (3/1 mol/mol) (gray bars), and POPC (white bars) after 1 min. The lipid concentration, c_l, was 25 μM, and the peptide concentration, c_p, was 10 μM in buffer (10 mM Tris, 154 mM NaCl, 0.1 mM EDTA, pH 7.4).

Table 2: Bilayer-Permeabilizing Activity of RW and c-RW[a]

	EC_{25} (μM)		
lipid (mol/mol)	RW	c-RW	EC_{25RW}/EC_{25c-RW}
POPC	4	1	4.0
POPC/POPG (3/1)	40	15	3.7
POPC/POPG (1/1)	160	40	4.0
POPC/POPG (1/3)	25	24	1.0
POPG	6.5	7.5	0.9

[a] EC_{25} gives the peptide concentration inducing 25% dequenching of the fluorescence of calcein entrapped in LUVs of different lipid compositions after 5 min. The lipid concentration was 25 μM. The quotient EC_{25RW}/EC_{25c-RW} is a measure for cyclization-induced improvement of the bilayer-permeabilizing activity.

tides (*38*). The change in t_R of the linear peptides, which followed the order RNal > RW = rw > KW > RY, reflected changes in the total hydrophobicity as a result of amino acid exchange. According to the octanol/water partition coefficient of the aromatic and charged residues, the hydrophobicities follow the orders Nal > W > Y and K > R, respectively (*39*). Upon cyclization, t_R of the W-bearing peptides increased. This increase might be related to an enhanced hydrophobicity as determined on the basis of the "hydrophobic fragment constant" approach (*40*), but also pointed to a clustering of hydrophobic residues and an enhanced amphathicity of the cyclic compounds.

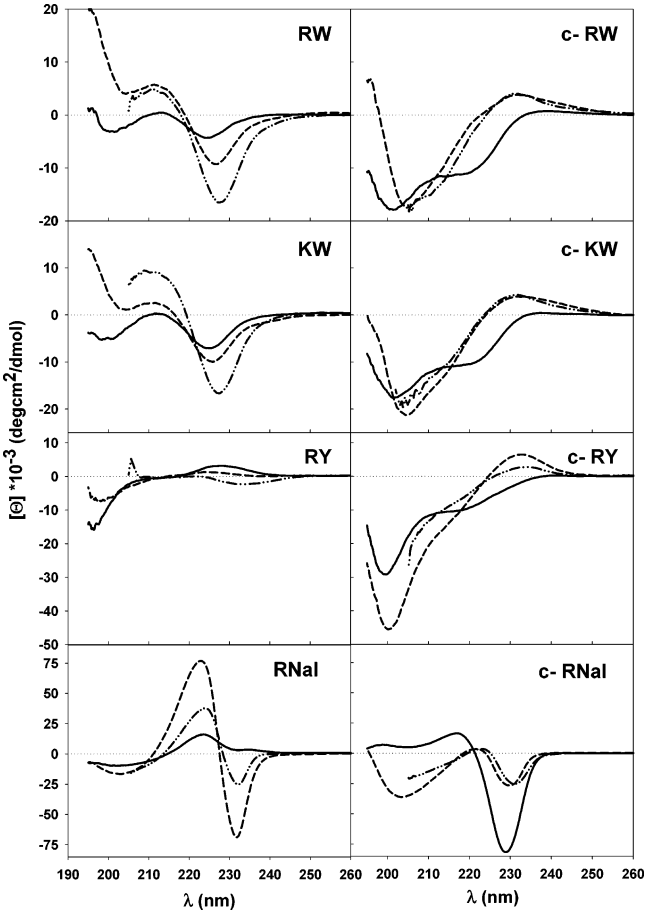

FIGURE 4: CD characteristics of linear and cyclic hexapeptides. Shown are the CD spectra of the linear RW, KW, RY, and RNal peptides and the corresponding cyclic compounds c-RW, c-KW, c-RY, and c-RNal in buffer (solid line), in the presence of SDS micelles (dashed line) and POPG SUVs (dashed−dotted line). [Θ] represents the mean residue ellipticity. The concentration of peptides dissolved in buffer (10 mM Tris, 154 mM NaF, 0.1 mM EDTA, pH 7.4), c_p, was 100 μM, the SDS concentration was 25 mM, and the lipid concentration, c_l, was 10 mM.

Peptide Structure Determined by CD Spectroscopy. The spectra of the W-containing linear peptides RW and KW dissolved in buffer showed two negative bands at 200 and 225 nm (Figure 4). The negative band at 200 nm is characteristic of small random coil peptides, and the band at 225 nm is probably due to the dichroism of the W residues (*41*, *42*). Addition of vesicles impaired CD spectroscopy at wavelengths shorter than 205 nm. Nevertheless, the increase and shift of the negative band to 229 nm and the positive ellipticity values at lower wavelengths upon partitioning of RW and KW into SDS micelles and POPG vesicles implied restrictions in the backbone structure and changes in the environment of the aromatic residues as suggested by studies of gramicidins (*43*) and indolicidin (*42*). The spectra of the cyclic analogues c-RW, c-KW, and c-RY in buffer showed a negative band at 200 nm and a shoulder at about 220 nm. The maximum at 230 nm in the micelle- and vesicle-bound states pointed to distinct changes in the orientation of the aromatic side chains relative to the peptide backbone (*41*). Although it is difficult to deconvolute the CD spectra of the cyclic peptides unambiguously because of the various contributions of turns and aromatic residues, it is reasonable to conclude that the more constrained cyclic analogues

Table 3: Quenching of the Tryptophan Fluorescence of RW and c-RW by Acrylamide[a]

		linear									cyclic								
		POPC			POPC/POPG (3/1 mol/mol)			POPG			POPC			POPC/POPG (3/1 mol/mol)			POPG		
peptide	c_l/c_p	λ (nm)	K_{SV} (M^{-1})	f	l	K_{SV} (M^{-1})	f	λ (nm)	K_{SV} (M^{-1})	f	λ (nm)	K_{SV} (M^{-1})	f	λ (nm)	K_{SV} (M^{-1})	f	λ (nm)	K_{SV} (M^{-1})	f
RW	0	354	12.2	1	354	12.5	1	355	12.1	1	352	13.9	1	354	15.1	1	354	14.5	1
	50	351	15.2	0.99							349	9.6	0.81						
	200	346	8.2	0.88	339	6.2	0.6	339	5.6	0.45	348	9.0	0.65	344	6.4	0.45	345	8.0	0.22
	500	344	8.2	0.75							344	10.5	0.48						
rw	0	354	11.9	1				354	11.2	1	354	13.4	1				353	13.4	1
	50	350	12.5	0.94							349	11.9	0.86						
	200	346	8.3	0.90				341	5.1	0.47	345	8.7	0.7				344	7.6	0.29
	500	344	8.4	0.79							344	9.3	0.54						

[a] Quenching constants (K_{SV}) and the fraction of peptide (f) accessible to the quencher acrylamide. The data were evaluated by curve fitting using the equation $F_o/F - 1 = (K_{SV}c_q f)/(1 + K_{SV}c_q(1 - f))$ (*32*). F_o/F is the ratio of the fluorescence intensity of the sample without the quencher to that at quencher concentration c_q. c_l/c_p denotes the ratio of lipid to peptide concentration. c_p was 5 μM. λ gives the wavelength of the emission maximum.

displayed some degree of an ordered structure in solution with further reduction in the number of backbone conformers and a well-defined orientation of aromatic side chains in the vesicle-bound state. The increase of the negative band of RNal in the presence of SDS and POPG at 232 nm was coupled to the maximum at 222 nm. Such a behavior is expected to result from exciton splitting. If two identical chromophores are sufficiently close, the excited states will interact and can make large contributions to the CD of peptides and proteins (*44*). The two components of the characteristic band called a couplet have the same magnitude but opposite signs. A comparison of the spectrum of RNal in buffer and in the presence of vesicles and micelles revealed a difference spectrum with the shape of a couplet centered at 227 nm, thus pointing to a stacking of the bulky aromatic residues in the bound state.

Fluorescence Spectroscopy. To examine the location of the lipid-bound peptides, we determined the tryptophan fluorescence spectra and investigated the effect of the water-soluble quencher acrylamide. W residues fully exposed to an aqueous environment have maxima above 350 nm, and those that are partially or completely buried have maxima below 345 and 330 nm, respectively (*45*). The fluorescence spectra of buffer-dissolved RW-containing peptides and their all-D analogues were characterized by an emission maximum at 354 ± 1 nm (Table 3). The blue shift to 344 nm (Table 3) as well as the increase in fluorescence intensity (not shown) upon increasing the POPC to peptide ratio to 500 correlated with a transfer of the peptides from the aqueous into the lipid environment. The data in Table 3 suggest that linear and cyclic compounds assumed comparable positions in the POPC bilayer. Slight differences in the depth of insertion seemed to exist between linear and cyclic peptides bound to POPG and POPC/POPG bilayers. Fluorescence maxima between 339 and 341 nm for the linear RW peptides pointed to a more distant position of W from the bilayer surface compared to that of the cyclic analogues with λ_{max} at 344 nm.

In the lipid environment, the accessibility of the W residues to an aqueous quencher should be reduced. Typically, fully exposed W residues have Stern−Volmer quenching constants, K_{SV}, of 8−9 M^{-1} (*46*), whereas K_{SV} for inaccessible W can be close to 0 M^{-1} (*47*). For data evaluation we used the linear part of the quenching curve. In our experiments the fluorescence data could be adequately fitted with a two-state model of quencher-accessible and -inaccessible chromophore. K_{SV} values of about 12 and 14 M^{-1} determined for the linear and cyclic RW peptides dissolved in buffer, respectively (Table 3), have also been reported for indolicidin and lactoferricin peptides (*48*). The affinity of the linear RW to POPC bilayers was low as shown by the fraction of 0.75−0.79 of free peptide at a POPC/peptide ratio of 500. Cyclization enhanced the affinity. Values below 0.5 for the quencher-accessible peptide fraction in the presence of mixed POPC/POPG and pure POPG vesicles suggested that peptide accumulation distinctly increased with the negative bilayer charge and was much more pronounced for the POPG-bound cyclic analogues.

Isothermal Titration Calorimetry. Peptide binding was further analyzed by titration calorimetric studies. Figure 5A demonstrates that the exothermic heat flow decreased with increasing number of injections of c-RW, since less and less peptide was available for binding. The corrected heats of reaction of c-RW and RW are given in Figure 5B. Thermodynamic parameters are summerized in Table 4. Binding of RW to POPC SUVs was characterized by an enthalpy $\Delta H = -12$ kcal/mol. The free energy of partitioning, $\Delta G°$, was calculated to be −8.8 kcal/mol, and the hydrophobic partition coefficient, K, was 4000 M^{-1}. ΔH was more negative than $\Delta G°$, implying a negative entropy change, $\Delta S°$. Thus, insertion of the linear peptide into the neutral lipid layer was driven by enthalpy and opposed by entropy. Binding of the small cationic peptides to lipid vesicles was an enthalpy-driven reaction comparable to those reported for helical antimicrobial peptides such as magainin (*36*) or the cyclic peptide somatostatin and its analogues (*34*). The thermodynamic parameters were consistent with a nonclassical hydrophobic effect (*49*). A slight gain in free energy and an increased partition coefficient showed that membrane binding was facilitated by cyclization. Whereas the negative enthalpy change decreased due to the restricted conformation, the entropy change became positive, showing that partitioning of cyclic peptides into the lipid layer was entropically favorable. Substitution of W by the more hydrophobic Nal further enhanced peptide affinity, whereas R−K exchange reduced partitioning into the POPC bilayer. Signals of the titration curves of RY and c-KY were too weak for deriving binding parameters. Interestingly, the intrinsic partition coefficients were reduced by increasing the negative bilayer charge as reflected by partition coefficients of 800 and 2500

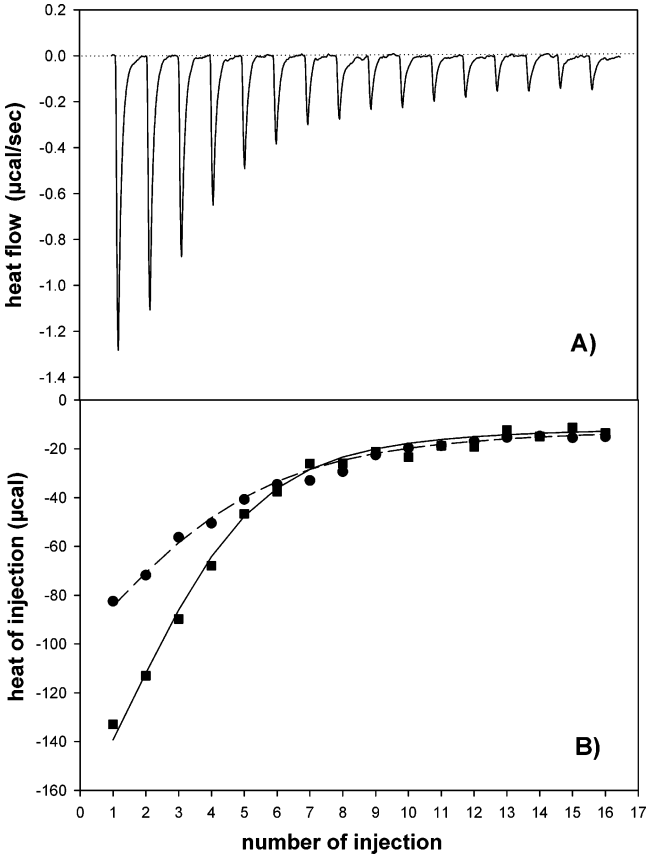

FIGURE 5: Titration calorimetry of RW and c-RW solutions (c_p = 40 μM) with a POPC SUV suspension (c_l = 44 mM) at 25 °C. (A) Calorimetric traces of c-RW. Each peak corresponds to the injection of 10 μL of lipid suspension into the reaction cell. (B) Heat of reaction as a function of the injection number obtained by integration of calorimetric traces of RW (circles) and c-RW (squares). The heat of dilution was measured in separate experiments and subtracted. The fitting curves were calculated by combining the surface partition equilibrium with the Gouy−Chapman theory. The binding constants used for the calculation are given in Table 4.

Table 4: Thermodynamic Parameters for Peptide Binding to POPC SUVs[a]

	POPC				
peptide	ΔH (kcal/mol)	$\Delta G°$ (kcal/mol)	$\Delta S°$ (cal/(mol K))	$-T\Delta S°$ (kcal/mol)	K (M^{-1})
RW	−12	−8.8	−10.7	3.2	4000
c-RW	−8.4	−9.4	3.4	−1.0	10000
c-RNal	−7.4	−10.3	9.7	−2.9	32000
c-KW	−6.7	−9.1	8.0	−2.4	6000

[a] ΔH values were calculated from the sum of corrected heats of reaction. Typically, 10 μL of the POPC SUV suspension (c_l = 44 mM) was injected into a 40 μM peptide solution at 25 °C. Changes in free energies ($\Delta G°$) and entropies ($\Delta S°$) were calculated using the equations $\Delta G° = -RT \ln 55.5K$ and $\Delta G° = \Delta H° - T\Delta S°$. The hydrophobic partition coefficient (K) was derived taking into consideration electrostatic peptide−bilayer interaction with the Gouy−Chapman theory. Assuming that the cationic peptides cannot cross the bilayer, only the lipid in the outer half of the layer was considered for the calculation of the binding parameters.

M^{-1} for RW and c-RW in mixed POPC/POPG (3/1 mol/mol) vesicles, respectively.

Measurement of Depth of Insertion. To determine the depth of insertion of RW and c-RW into lipid bilayers, fluorescence quenching experiments using *n*-doxyl-PCs (TEMPO, 5-DOX, 12-DOX) were carried out. The parallax analysis is most accurate when the chromophore is close to the quencher (*50*). Figure 6 illustrates distinct differences in the quenching efficiency of TEMPO- and 12-DOX-labeled lipids on POPC-bound c-RW. The tryptophan fluorescence of RW and c-RW bound to POPC vesicles was most strongly quenched by 5-DOX and 12-DOX (Table 5). This result is in accordance with quenching studies of indolicidin (*51*) and an indolicidin analogue (*52*). With the negatively charged POPC/POPG system the differences in the quenching ability of the three doxyl labels were less pronounced, and the strongest quenching was found with TEMPO- and 5-DOX-PC (Table 5). The calculated distances of W (z_{cf}) from the bilayer center clearly show that RW and c-RW were deeply inserted and have the same position in the POPC bilayer, whereas the peptides bound to the negatively charged POPC/POPG layers were located next to the headgroup acyl chain interface (Figure 7).

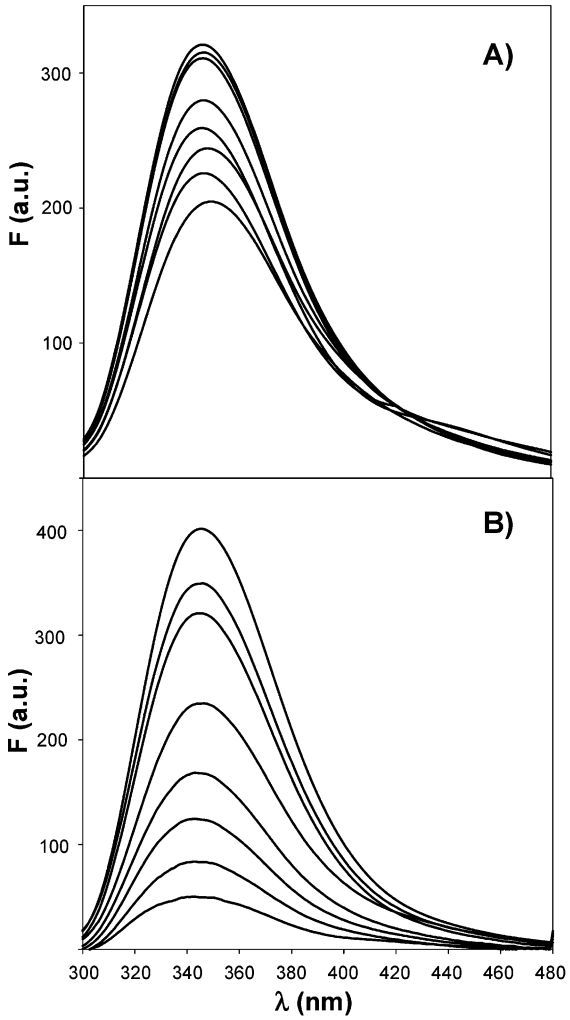

FIGURE 6: Fluorescence spectra of c-RW bound to POPC vesicles containing (A) TEMPO- and (B) 5-DOX-labeled lipids. The peptide concentration, c_p, was 2 μM, the lipid concentration, c_l, was 400 μM, and the fraction of spin-labeled lipid was 0, 2.2, 5.4, 10.3, 14.4, 20.2, 31.4, and 40.3 mol % from the top to the bottom.

DISCUSSION

The new finding of this work was that cyclization of the W- and R-containing hexapeptides had a pronounced anti-

Table 5: Quenching of Tryptophan Fluorescence by Nitroxide-Labeled Lipids and Distances between Tryptophan and the Bilayer Center[a]

	POPC				POPC/POPG (3/1 molar ratio)			
	S			z_{cf} (Å)	*S*			z_{cf} (Å)
peptide	TEMPO	5-DOX	12-DOX	5-DOX/12-DOX	TEMPO	5-DOX	12-DOX	TEMPO/5-DOX
RW	−1.26	−7.88	−7.12	10.3	−4.04	−4.09	−3.12	15.6
	−1.02	−7.15	−5.79	12.4				
c-RW	−1.67	−5.74	−5.29	9.4	−3.08	−3.51	−2.57	15.2
	−1.59	−6.88	−6.65	9.6				

[a] *S* is the slope of the plot of ln F/F_o vs the mole fraction of lipids carrying spin-labels 19.5 Å (TEMPO) (*31*), 12.2 Å (5-DOX), and 5.85 Å (12-DOX) (*30*) from the bilayer center. F/F_o is the ratio of W fluorescence intensity in POPC and POPC/POPG (3/1 molar ratio) vesicles containing the quencher to that of vesicles without the quencher. The mole fraction of spin-labeled lipid ranged from 0 to 0.4. The peptide concentration c_p was 2 μM, the lipid concentration c_l was 400 μM. The distance (z_{cf}) between the fluorescent groups of RW and the cyclic analogue c-RW and the bilayer center calculated by applying the parallax equation to tryptophan emission was determined for labels closest to the aromatic residue.

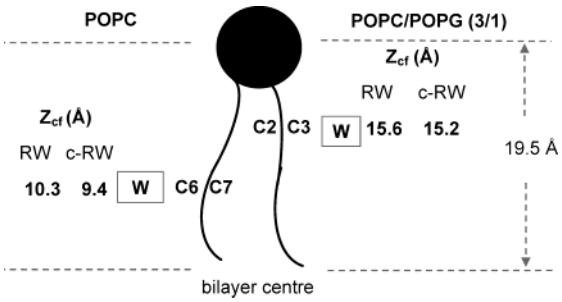

FIGURE 7: Schematic illustration of the location of tryptophan W of RW and c-RW in lipid layers composed of POPC and mixed POPC/POPG (3/1 mol/mol). z_{cf} is the distance of the aromatic residue from the bilayer center (lower dashed line). The upper dashed line delineates the distance of the nitroxide label in the lipid headgroup from the bilayer center. C6, C7 and C2, C3 denote the carbon atoms of the acyl chains next to the inserted W residue.

microbial activity- and selectivity-enhancing effect. Studies with tyrosine- or naphthylalanine-bearing peptides demonstrated that the conformation-based effect was restricted to sequences of an appropriate hydrophobicity. Furthermore, we found that the activity-improving effect of cyclization was counteracted by high negative charge on lipid bilayers and the bacterial target membrane.

Since the small peptides composed of L-amino acid residues and their all-D enantiomers exhibited identical biological activity patterns, interactions with the lipid matrix of the cell membrane might play an important role. Elucidation of the mode of action on the biological level will require an understanding of how the peptides interact with the lipid matrix. Recent studies on helical amphipathic peptides resulted in a model of peptide−lipid interactions that explains peptide activity as a function of the number of surface-accumulated peptides and their depth of insertion into the lipid matrix (*22*, *23*). Thus, we analyzed the relationship between the structure and the biological activity of small hexapeptides and put the results into relation to their bilayer-permeabilizing activity, binding behavior, and location in model membranes.

Peptide interactions with micelles and liposomes were indicated by distinct CD spectroscopic changes. The linear peptides apparently underwent a disordered−ordered transition while approaching the membrane. This is in accordance with the induction of an amphipathic structure of SDS-bound AcRRWWRF-NH_2 as derived from NMR studies (*53*). Changes in the environment of the chromophores associated with the formation of a hydrophobic cluster became evident with the cyclic peptides c-RW, c-KW, and c-RY in the presence of micelles and vesicles. Comparable CD spectra have been reported for lipid-bound analogues of tachyplesin, an amphipathic antiparallel β-sheet structure, where the charged residues are distributed around the molecule and aromatic residues are coordinated to a hydrophobic domain (*54*). Our suggestion of pronounced amphipathicity in the cyclic hexapeptides was supported by nuclear magnetic resonance (NMR) studies which showed that the structure of micelle-bound c-RW was characterized by a polar face consisting of the backbone ring and the charged residues and the aromatic side chains clustered opposite the ring plane (Appelt et al., PDB codes 1QVL and 1QVK, release on publication).

Similar structural properties of c-RW, c-KW, and c-RY but very different activities imply that an amphipathic nature of a peptide alone is not sufficient for activity. Our fluorescence spectroscopic studies showed that binding of linear and cyclic RW peptides increased with enhancement of the negative bilayer charge. Since all peptides carry the same positive net charge, the favored accumulation of the cyclic analogues on negatively charged bilayers could be explained with an enhanced charge density. For helical model peptides it has been found that the apparent binding constant to pure POPG bilayers increased upon increasing the charge density by reducing the size of the charged helix surface (*23*). The gradual increase of the retention times of peptides with substitution of Y by W or Nal and exchange of K by R illustrated the importance of hydrophobicity for interaction with membrane-mimicking surfaces. Furthermore, the higher amount of bound c-RW and c-rw in the presence of neutral POPC vesicles compared to the linear analogues pointed to an enhanced contribution of hydrophobic interactions which was most likely based on clustering of the aromatic residues. This affinity-enhancing effect of cyclization and the activity-modulating role of peptide hydrophobicity were confirmed by titration calorimetric measurements. Partitioning of the linear RW was driven by a large negative enthalpy change. For conformationally constrained cyclic analogues the enthalpic contribution to the free energy of binding slightly decreased, but the loss in negative binding enthalpy was compensated by the gain in entropy, which favored partitioning into the lipid layer. The reduction in partitioning of RW peptides to negatively charged bilayers suggested that insertion with the hydrophobic side chains was reduced. Charge−charge interactions could position the peptide in the surface region of the lipid layer as reported for magainin

(*36*). An interfacial location where the linear RW interacts preferentially with the polar headgroups and the glycerol backbone region of the lipid bilayer is supported by differential calorimetric studies, which demonstrate that the peptide interacts more strongly with negative phosphatidylglycerols than zwitterionic phospholipids and decreases the temperature of the main phase transition (*53*). Quenching studies with internal lipid spin labels confirmed that investigated RW peptides were inserted into the hydrocarbon core of neutral bilayers and located next to polar headgoups in negatively charged model membranes. The position was independent of the peptide structure. An identical bilayer location derived from quenching studies has also been suggested for other conformationally different RW-rich peptides such as tritrpticin, indolicidin, and the lactoferricin-derived hexapeptide (*48*).

Bilayer permeabilization has been described to be determined by two components: peptide accumulation, which is distinctly enhanced by electrostic interactions, and the permeabilizing efficiency determined by hydrophobic interactions (*23*). The pronounced activity of our RW peptides toward highly negatively charged POPG bilayers supports an idea of rapid bilayer disruption to reduce the tension in the outer leaflet caused by a high amount of peptide accumulated in the surface (*55*). Reduced conformational flexibility and lower reorientation rates of the space-consuming cyclic peptides might be responsible for their slower permeabilization kinetics. On neutral POPC bilayers high peptide hydrophobicity or the formation of hydrophobic domains favored peptide partitioning into the nonpolar bilayer region. Although peptide accumulation was low, penetration of the RW-containing peptides into the acyl chain region caused an effective disruption. The constrained cyclic compound was most effective in disturbing the packing of lipid chains. The low activity of our peptides toward mixed POPC/POPG bilayers can be associated with a lower amount of bound peptides compared to POPG. Furthermore, their fixation in the bilayer surface reduced the permeabilizing efficiency. This effect of shallow insertion could partially be compensated by the rigid structure of the cyclic peptide. The observation of comparable location but different activity of the linear and cyclic RW peptides is in accordance with reports on comparable location of other RW-containing peptides different in size and conformation with very different permeabilizing activities. It has been suggested that the more potent peptides are those that appear to be more rigid (*48*). Amphipathicity caused by clustering of Y was not strong enough to induce activity, and in the case of Nal-containing peptides, the effect of stacking of the aromatic residues was superimposed by the high global hydrophobicity. Thus, there seems to exist a hydrophobicity window in which the activity of appropriate short sequences can be enhanced by cyclization.

The activity-enhancing effect of cyclization was most pronounced with bacteria but only moderate with red blood cells. Thus, cyclization distinctly enhanced the bacterial selectivity. The membrane of red blood cells is composed of electrically neutral lipids. The peptide activity was determined by hydrophobicity and slightly improved by cluster formation of the aromatic residues in the cyclic analogues. The role of hydrophobicity and amphipathicity was also reflected with bacterial membranes. Modified activities upon amino acid substitution are in accordance with results of other R- and W-rich peptides such as lactoferricin sequences (*8*, *56*,) and hexapeptides derived from a combinatorial library (*57*). The discrepancy between values greater than 8 for the quotient MIC_l/MIC_c (Figure 1) illustrating the cyclization-based improvement of antimicrobial activity of our parent peptide and EC_{25RW}/EC_{25c-RW} values lower than 4 (Table 2) for cyclication-enhanced bilayer permeabilization has to be related to the complexity of the cell membranes. The cytoplasmic membrane of *E. coli* is surrounded by a highly negatively charged lipopolysaccharide (LPS)-rich outer wall. The sequences examined in this study show a feature that is characteristic of LPS-binding motifs: two positively charged amino acid residues separated from the third by a short hydrophobic, aromatic stretch. Structurally related LPS-binding motifs have been found within the bactericidal permeability-increasing protein (*58*) and lactoferricin (*59*). Thus, facilitated "self-promoted uptake" (*2*) may lead to an improved accessibility of the cyclic peptides to the inner target membrane. On the slightly negatively charged target membrane, R and W confer significant affinity and perturbing ability on the cyclic peptides. The lower MIC_l/MIC_c values found for *B. subtilis* compared to *E. coli* could be caused by the high amount of negatively charged lipids being in the range of 75% (*60*) and 25%, respectively (*61*). As our studies on model membranes demonstrated, the activity-enhancing effect of cyclization disappeared at high negative bilayer charge.

Since the tryptophan residues partition into negatively charged membranes preferentially at the interface, neither the linear nor cyclic peptides would be expected to span the bilayer or to form channels. A recently described RW-containing cyclic D,L-α-peptide displays potent and selective antimicrobial activity and a low level of hemolysis. But unlike the peptides investigated in this study, the orientation of the flat backbone ring and the side chains in a plane allows these peptides to form associates of tubular structures which could insert into the membrane (*62*). Instead, our highly active cyclic RW peptide may cause membranes to become leaky by increasing the lateral pressure in the bilayer, which could lead to a transient disturbance of the barrier function.

In summary we found that cyclization confers high antimicrobial activity and selectivity on arginine- and trypophan-rich hexapeptides. The studies lead to the suggestion that the induced activity and selectivity of the rigid peptides is based on structural principles similar to those derived for larger cationic amphipathic helices. The interaction of the peptides with lipid matrixes of the target membranes could be described by a sensitive balance of electrostatic and hydrophobic interactions. Interactions with specific components of the biological cells such as the lipopolysaccharides of the outer *E. coil* wall, which are currently under detailed investigation, might modify their effect. The appropriate balance between global hydrophobicity of RW-containing sequences and the amphipathicity generated by conformational constraints might also endow larger peptides with antimicrobial activity and selectivity. With their low molecular weight and an improved enzymatic stability reported for cyclic compounds, our RW-rich peptides offer an attractive complement to the current spectrum of antimicrobial peptides and might be promising lead structures for prospective antibiotic agents.

ACKNOWLEDGMENT

The invaluable help of H. Hans, Dr. M. Beyermann, A. Ehrlich, A. Wessolowki, and B. Schmikale in the synthesis of peptides and of D. Krause, Dr. M. Schümann, and H. Lerch in peptide purification and mass spectrometric analysis is gratefully acknowledged. S. Keller is thanked very much for his support with ITC measurements and for critically reading the manuscript.

REFERENCES

1. Zasloff, M. (2002) Antimicrobial peptides of multilamellar organisms, *Nature 415*, 389−395.
2. Hancock, R. E. (1997) Peptide antibiotics, *Lancet 349*, 418−422.
3. Bechinger, B. (1999) The structure, dynamics and orientation of antimicrobial peptides in membranes by multidimensional solid-state NMR spectroscopy, *Biochim. Biophys. Acta 1462*, 157−183.
4. Tomita, M., Takase, M., Bellamy, W., and Shimamura, S. (1994) A review: the active peptide of lactoferrin, *Acta Paediatr. Jpn. 36*, 585−591.
5. Staubitz, P., Peschel, A., Nieuwenhuizen, W. F., Otto, M., Gotz, F., Jung, G., and Jack, R. W. (2001) Structure−function relationships in the tryptophan-rich, antimicrobial peptide indolicidin, *J. Pept. Sci. 7*, 552−564.
6. Nagpal, S., Gupta, V., Kaur, K. J., and Salunke, D. M. (1999) Structure−function analysis of tritrypticin, an antibacterial peptide of innate immune origin, *J. Biol. Chem. 274*, 23296−23304.
7. Blondelle, S. E., Takahashi, E., Dinh, K. T., and Houghten, R. A. (1995) The antimicrobial activity of hexapeptides derived from synthetic combinatorial libraries, *J. Appl. Bacteriol. 78*, 39−46.
8. Strom, M. B., Rekdal, O., and Svendsen, J. S. (2002) Antimicrobial activity of short arginine- and tryptophan-rich peptides, *J. Pept. Sci. 8*, 431−437.
9. Strom, M. B., Haug, B. E., Skar, M. L., Stensen, W., Stiberg, T., and Svendsen, J. S. (2003) The pharmacophore of short cationic antibacterial peptides, *J. Med. Chem. 46*, 1567−1570.
10. Muta, T., Fujimoto, T., Nakajima, H., and Iwanaga, S. (1990) Tachyplesins isolated from hemocytes of Southeast Asian horseshoe crabs (Carcinoscorpius rotundicauda and Tachypleus gigas): identification of a new tachyplesin, tachyplesin III, and a processing intermediate of its precursor, *J. Biochem. (Tokyo) 108*, 261−266.
11. Nakamura, T., Furunaka, H., Miyata, T., Tokunaga, F., Muta, T., Iwanaga, S., Niwa, M., Takao, T., and Shimonishi, Y. (1988) Tachyplesin, a class of antimicrobial peptide from the hemocytes of the horseshoe crab (Tachypleus tridentatus). Isolation and chemical structure, *J. Biol. Chem. 263*, 16709−16713.
12. Vogel, H. J., Schibli, D. J., Jing, W., Lohmeier-Vogel, E. M., Epand, R. F., and Epand, R. M. (2002) Towards a structure−function analysis of bovine lactoferricin and related tryptophan- and arginine-containing peptides, *Biochem. Cell Biol. 80*, 49−63.
13. Haug, B. E., Skar, M. L., and Svendsen, J. S. (2001) Bulky Aromatic Amino Acids Increase the Antibacterial Activity of 15-Residue Bovin Lactoferricin Derivatives, *J. Pept. Sci. 7*, 425−432.
14. Wu, M. H., and Hancock, R. E. W. (1999) Improved derivatives of bactenecin, a cyclic dodecameric antimicrobial cationic peptide, *Antimicrob. Agents Chemother. 43*, 1274−1276.
15. Kokryakov, V. N., Harwig, S. S., Panyutich, E. A., Shevchenko, A. A., Aleshina, G. M., Shamova, O. V., Korneva, H. A., and Lehrer, R. I. (1993) Protegrins: leukocyte antimicrobial peptides that combine features of corticostatic defensins and tachyplesins, *FEBS Lett. 327*, 231−236.
16. Romeo, D., Skerlavaj, B., Bolognesi, M., and Gennaro, R. (1988) Structure and bactericidal activity of an antibiotic dodecapeptide purified from bovine neutrophils, *J. Biol. Chem. 263*, 9573−9575.
17. Agerberth, B., Lee, J. Y., Bergman, T., Carlquist, M., Boman, H. G., Mutt, V., and Jornvall, H. (1991) Amino acid sequence of PR-39. Isolation from pig intestine of a new member of the family of proline-arginine-rich antibacterial peptides, *Eur. J. Biochem. 202*, 849−854.
18. Kang, J. H., Lee, M. K., Kim, K. L., and Hahm, K. S. (1996) Structure-biological activity relationships of 11-residue highly basic peptide segment of bovine lactoferrin, *Int. J. Pept. Protein Res. 48*, 357−363.
19. van't Hof, W., Veerman, E. C. I., Helmerhorst, E. J., and Nieuw Amerongen, A. V. (2001) Antimicrobial Peptides: Properties and Applikation, *Biol. Chem. 382*, 597−619.
20. Hwang, P. M., Zhou, N., Shan, X., Arrowsmith, C. H., and Vogel, H. J. (1998) Structure−function relationships of antimicrobial peptides, *Biochemistry 37*, 4288−4298.
21. Schibli, D. J., Hwang, P. M., and Vogel, H. J. (1999) The structure of the antimicrobial active center of lactoferricin B bound to sodium dodecyl sulfate micelles, *FEBS Lett. 446*, 213−217.
22. Dathe, M., Schümann, M., Wieprecht, T., Winkler, A., Beyermann, M., Krause, E., Matsuzaki, K., Murase, O., and Bienert, M. (1996) Peptide helicity and membrane surface charge modulate the balance of electrostatic and hydrophobic interactions with lipid bilayers and biological membranes, *Biochemistry 35*, 12612−12622.
23. Dathe, M., Meyer, J., Beyermann, M., Maul, B., Hoischen, C., and Bienert, M. (2002) General aspects of peptide selectivity towards lipid bilayers and cell membranes studied by variation of the structural parameters of amphipathic helical model peptides, *Biochim. Biophys. Acta 1558*, 171−186.
24. Dathe, M., Nikolenko, H., Beyermann, M., and Bienert, M. (2002) Cyclization increases the antimicrobial activity and selectivity of tryptophan and arginine containing hexapeptides, *Biophys. J. 82*, 561a.
25. Beyermann, M., and Bienert, M. (1992) Synthesis of difficult peptide sequences: a comparison of Fmoc- and Boc-technique, *Tetrahedron Lett. 33*, 3745−3748.
26. Ehrlich, A., Heyne, H.-U., Winter, R., Beyermann, M., Carpino, L. A., and Bienert, M. (1996) Rapid cyclization on all-L-pentapeptides by means of 1-hydroxy-7-azabenzotriazole-derived uronium and phosphonium reagents, *J. Org. Chem. 61*, 8831−8838.
27. New, R. B. C. (1990) Characterization of liposomes, in *Liposomes a practical approach* (New, R. R. C., Ed.) pp 105−161, IRL Press/Oxford University Press, Oxford.
28. Böttcher, C. J. F., Van Gent, C. M., and Pries, C. (1961) A rapid and sensitive sub-micro phosphorus determination, *Anal. Chim. Acta 24*, 203−204.
29. London, E., and Feigenson, G. W. (1981) Fluorescence quenching in model membranes. 1. Characterization of quenching caused by a spin-labeled phospholipid, *Biochemistry 20*, 1932−1938.
30. Chattopadhyay, A., and London, E. (1987) Parallax method for direct measurement of membrane penetration depth utilizing fluorescence quenching by spin-labeled phospholipids, *Biochemistry 26*, 39−45.
31. Abrams, F. S., and London, E. (1993) Extension of the parallax analysis of membrane penetration depth to the polar region of model membranes: use of fluorescence quenching by a spin-label attached to the phospholipid polar headgroup, *Biochemistry 32*, 10826−10831.
32. Talbot, J. C., Thiaudiere, E., Vincent, M., Gallay, J., Siffert, O., and Dufourcq, J. (2001) Dynamics and orientation of amphipathic peptides in solution and bound to membranes: a steady-state and time-resolved fluorescence study of staphylococcal delta-toxin and its synthetic analogues, *Eur. Biophys. J.* 147−161.
33. Seelig, J. (1997) Titration calorimetry of lipid-peptide interactions, *Biochim. Biophys. Acta 1331*, 103−116.
34. McLaughlin, S. (1989) The electrostatic properties of membranes, *Annu. Rev. Biophys. Biophys. Chem. 18*, 113−136.
35. Seelig, J., Nebel, S., Ganz, P., and Bruns, C. (1993) Electrostatic and nonpolar peptide-membrane interactions. Lipid binding and functional properties of somatostatin analogues of charge $z = +1$ to $z = +3$, *Biochemistry 32*, 9714−9721.
36. Wieprecht, T., Beyermann, M., and Seelig, J. (1999) Binding of antibacterial magainin peptides to electrically neutral membranes: thermodynamics and structure, *Biochemistry 38*, 10377−10387.
37. Krause, E., Beyermann, M., Dathe, M., Rothemund, S., and Bienert, M. (1995) Location of an amphipathic alpha-helix in peptides using reversed-phase HPLC retention behavior of D-amino acid analogs, *Anal. Chem. 67*, 252−258.
38. Kondejewski, L. H., Jelokhani Niaraki, M., Farmer, S. W., Lix, B., Kay, C. M., Sykes, B. D., Hancock, R. E. W., and Hodges, R. S. (1999) Dissociation of antimicrobial and hemolytic activities in cyclic peptide diastereomers by systematic alterations in amphipathicity, *J. Biol. Chem. 274*, 13181−13192.

39. Fauchere, J. L., Charton, M., Kier, L. B., Verloop, A., and Pliska, V. (1988) Amino acid side chain parameters for correlation studies in biology and pharmacology, *Int. J. Pept. Protein Res. 32*, 269−278.
40. Black, S. D., and Mould, D. R. (1990) Development of hydrophobicity parameters to analyze proteins which bear post- or cotranslational modifications, *Anal. Biochem. 193*, 72−82.
41. Woody, R. W. (1994) Contributions of tryptophan side chains to the far-ultraviolet circular dichroism of proteins, *Eur. Biophys. J. 23*, 253−262.
42. Ladokhin, A. S., Selsted, M. E., and White, S. H. (1997) Bilayer interactions of indolicidin, a small antimicrobial peptide rich in tryptophan, proline, and basic amino acids, *Biophys. J. 72*, 794−805.
43. Woolley, G. A., Dunn, A., and Wallace, B. A. (1992) Gramicidin-lipid interactions induce specific tryptophan side-chain conformations, *Biochem. Soc. Trans. 20*, 864−867.
44. Grishina, I. B., and Woody, R. W. (1994) Contributions of tryptophan side chains to the circular dichroism of globular proteins: exciton couplets and coupled oscillators, *Faraday Discuss.* 245−262.
45. Burstein, E. A., Vendenkina, N. S., and Ivkova, M. N. (1973) Fluorescence and the location of tryptophan residues in protein molecules, *Photochem. Photobiol. 18*, 263−279.
46. Wimley, W. C., Creamer, T. P., and White, S. H. (1996) Solvation energies of amino acid side chains and backbone in a family of host−guest pentapeptides, *Biochemistry 35*, 5109−5124.
47. Liu, L. P., and Deber, C. M. (1997) Anionic phospholipids modulate peptide insertion into membranes, *Biochemistry 36*, 5476−5482.
48. Schibili, D. J., Epand, R. F., Vogel, H. J., and Epand, R. M. (2002) Tryptophan-rich antimicrobial peptides: comparative properties and membrane interactions, *Biochem. Cell Biol. 80*, 667−677.
49. Huang, C. H., and Charlton, J. P. (1972) Interactions of phosphatidylcholine vesicles with 2-p-toluidinylnaphthalene-6-sulfonate, *Biochemistry 11*, 735−740.
50. Ladokhin, A. S., and Holloway, P. W. (1995) Fluorescence of membrane-bound tryptophan octyl ester: a model for studying intrinsic fluorescence of protein-membrane interactions, *Biophys. J. 69*, 506−517.
51. Rozek, A., Friedrich, C. L., and Hancock, R. E. (2000) Structure of the bovine antimicrobial peptide indolicidin bound to dodecylphosphocholine and sodium dodecyl sulfate micelles, *Biochemistry 39*, 15765−15774.
52. Friedrich, C. L., Rozek, A., Patrzykat, A., and Hancock, R. E. (2001) Structure and mechanism of action of an indolicidin peptide derivative with improved activity against gram-positive bacteria, *J. Biol. Chem. 276*, 24015−24022.
53. Jing, W., Hunter, H. N., Hagel, J., and Vogel, H. J. (2003) Influence of tryptophan on lipid binding of linear amphipathic cationic antimicrobial peptides, *J. Pept. Res. 61*, 219−229.
54. Oishi, O., Yamashita, S., Nishimoto, E., Lee, S., Sugihara, G., and Ohno, M. (1997) Conformations and orientations of aromatic amino acid residues of tachyplesin I in phospholipid membranes, *Biochemistry 36*, 4352−4359.
55. Matsuzaki, K. (1999) Why and how are peptide-lipid interactions utilized for self-defense? Magainins and tachyplesins as archetypes, *Biochim. Biophys. Acta 1462*, 1−10.
56. Haug, B. E., and Svendsen, J. S. (2001) The role of tryptophan in the antibacterial activity of a 15-residue bovine lactoferricin peptide, *J. Pept. Sci. 7*, 190−196.
57. Blondelle, S. E., and Lohner, K. (2000) Combinatorial libraries: A tool to design antimicrobial and antifungal peptide analogues having lyric specificities for structure- activity relationship studies, *Bioplymers 55*, 74−87.
58. Little, R. G., Kelner, D. N., Lim, E., Burke, D. J., and Conlon, P. J. (1994) Functional domains of recombinant bactericidal/permeability increasing protein (rBPI23), *J. Biol. Chem. 269*, 1865−1872.
59. Elass-Rochard, E., Roseanu, A., Legrand, D., Trif, M., Salmon, V., Motas, C., Montreuil, J., and Spik, G. (1995) Lactoferrin-lipopolysaccharide interaction: involvement of the 28−34 loop region of human lactoferrin in the high-affinity binding to Escherichia coli 055B5 lipopolysaccharide, *Biochem. J. 312*, 839−845.
60. O'Leary, W. M., and Wilkinson, S. G. (1988) Gram-positive bacteria, in *Microbial lipids* (Ratledge, C., and Wilkinson, S. G., Eds.) pp 117−201, Academic Press Ltd., London.
61. Wilkinson, S. G. (1988) Gram-negative bacteria, in *Microbial lipids* (Ratledge, C., and Wilkinson, S. G., Eds.) pp 299−488, Academic Press Ltd., London.
62. Fernandez-Lopez, S., Kim, H.-S., Choi, E. C., Delgado, M., Granja, J. R., Khasanov, A., Kraehenbuehl, K., Long, G., Weinberger, D. A., Wilcoxen, K. M., and Ghadir M. R. (2001) Antibacterial agents based on the cyclic D,L-alpha-peptide architecture, *Nature 412*, 452−455.

BI035948V